

Symmetry considerations on the magnetization process of the Heisenberg model on the pyrochlore lattice

This article has been downloaded from IOPscience. Please scroll down to see the full text article.

2007 J. Phys.: Condens. Matter 19 145267

(<http://iopscience.iop.org/0953-8984/19/14/145267>)

View [the table of contents for this issue](#), or go to the [journal homepage](#) for more

Download details:

IP Address: 129.252.86.83

The article was downloaded on 28/05/2010 at 17:35

Please note that [terms and conditions apply](#).

Symmetry considerations on the magnetization process of the Heisenberg model on the pyrochlore lattice

Karlo Penc¹, Nic Shannon², Yukitoshi Motome³ and Hiroyuki Shiba⁴

¹ Research Institute for Solid State Physics and Optics, H-1525 Budapest, POB 49, Hungary

² H H Wills Physics Laboratory, Tyndall Avenue, Bristol BS8 1TL, UK

³ Department of Applied Physics, University of Tokyo, Bunkyo-ku, Tokyo 113-8656, Japan

⁴ The Institute of Pure and Applied Physics, 2-31-22 Yushima, Bunkyo-ku, Tokyo 113-0034, Japan

Received 27 September 2006

Published 23 March 2007

Online at stacks.iop.org/JPhysCM/19/145267

Abstract

We present a detailed symmetry analysis of the degeneracy lifting due to higher order spin exchanges in the pyrochlore lattice in applied magnetic field. Under the assumption of the four-sublattice ordering, the criteria for a stable half-magnetization plateau are deduced. The higher order exchange terms may originate from spin–lattice coupling, or can describe quantum and thermal fluctuations.

(Some figures in this article are in colour only in the electronic version)

1. Introduction

The very special feature of the antiferromagnetic nearest-neighbour Heisenberg model on a pyrochlore lattice is that it does not order magnetically at *any* temperature [1, 2]. This is a consequence of the high (continuous) degeneracy of its ground state manifold, which for $O(3)$ spins is too great even for order from disorder effects to be effective. Nonetheless, the vast majority of magnetic materials with a pyrochlore lattice *do* order magnetically. In these compounds, magnetic order is typically accompanied by a structural transition which lowers the crystal symmetry and so lifts the ground state degeneracy. This ‘order by distortion’ mechanism [3, 4] is a natural consequence of the magnetoelastic interactions present in almost all magnets. Examples may include YMn_2 [2, 5], $Y_2M_2O_7$ [6], but to date its most striking realization is in the high field properties of the chromium spinels $CdCr_2O_4$ [7] and $HgCr_2O_4$ [8].

In these compounds a dramatic half-magnetization plateau is accompanied by a colossal magnetostriction and change of crystal symmetry. The basic physics of this magnetization plateau can be understood by extending the simplest four-sublattice ‘order by distortion’ model of the pyrochlore lattice [3, 4] to finite magnetic field [9]. Here we develop a complete symmetry analysis of the most general four-sublattice order, and give additional details of the new phases which result when the assumptions made in [9] are relaxed to allow for more general spin–lattice interactions.

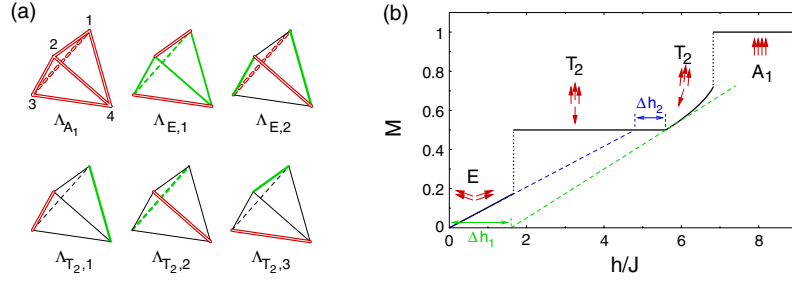


Figure 1. (a) Schematic representation of the different irreps of the tetrahedron. Hollow (red) lines have positive weight; thick (green) lines have negative weight; thin black lines have zero weight. (b) Magnetization curve for $b_{A_1} = 0.1$, $b_E = 0.1$ and $b_{T_2} = 0.2$. The spin configurations, together with the irreps they belong to, are indicated.

2. The effective model

We start by assuming a simplest microscopic form of magnetoelastic coupling, in which the strength of exchange interactions between a pair of nearest-neighbour classical spins (i, j) depends linearly on the change in length $\delta_{i,j}$ of the associated bond

$$\mathcal{H} = \sum_{(i,j)} \left[J(1 - \alpha \delta_{i,j}) \mathbf{S}_i \cdot \mathbf{S}_j + \frac{K}{2} \delta_{i,j}^2 \right] - h \sum_i S_i^z. \quad (1)$$

Here α is the spin–lattice coupling, and K an elastic coupling constant. We choose the z -axis to coincide with the direction of applied magnetic field. As the experiments point to an ordered state, we further assume that the simplest, four-sublattice order is stabilized, e.g. by longer range exchange interactions. Since we are interested in static quantities, we can then safely reduce the problem to that of a single tetrahedron embedded in a pyrochlore lattice⁵.

The symmetry group of this embedded tetrahedron is \mathcal{T}_d , which has 24 elements and 5 irreducible representations (irreps), see also figure 1(a). Bond variables such as $\delta_{i,j}$ and $\mathbf{S}_i \cdot \mathbf{S}_j$ transform according to the A_1 , E and T_2 irreps:

$$\begin{pmatrix} \Lambda_{A_1} \\ \Lambda_{E,1} \\ \Lambda_{E,2} \\ \Lambda_{T_2,1} \\ \Lambda_{T_2,2} \\ \Lambda_{T_2,3} \end{pmatrix} = \begin{pmatrix} \frac{1}{\sqrt{6}} & \frac{1}{\sqrt{6}} & \frac{1}{\sqrt{6}} & \frac{1}{\sqrt{6}} & \frac{1}{\sqrt{6}} & \frac{1}{\sqrt{6}} \\ \frac{1}{\sqrt{3}} & \frac{-1}{2\sqrt{3}} & \frac{-1}{2\sqrt{3}} & \frac{-1}{2\sqrt{3}} & \frac{-1}{2\sqrt{3}} & \frac{1}{\sqrt{3}} \\ 0 & \frac{1}{2} & \frac{-1}{2} & \frac{-1}{2} & \frac{1}{2} & 0 \\ 0 & 0 & \frac{-1}{\sqrt{2}} & \frac{1}{\sqrt{2}} & 0 & 0 \\ 0 & \frac{-1}{\sqrt{2}} & 0 & 0 & \frac{1}{\sqrt{2}} & 0 \\ \frac{-1}{\sqrt{2}} & 0 & 0 & 0 & 0 & \frac{1}{\sqrt{2}} \end{pmatrix} \begin{pmatrix} \mathbf{S}_1 \cdot \mathbf{S}_2 \\ \mathbf{S}_1 \cdot \mathbf{S}_3 \\ \mathbf{S}_1 \cdot \mathbf{S}_4 \\ \mathbf{S}_2 \cdot \mathbf{S}_3 \\ \mathbf{S}_2 \cdot \mathbf{S}_4 \\ \mathbf{S}_3 \cdot \mathbf{S}_4 \end{pmatrix}. \quad (2)$$

In this approach we assume that the spin-space and the real-space are decoupled, i.e. that the L – S coupling and crystalline anisotropies are negligible.

Under these assumptions, the Hamiltonian of the embedded tetrahedron is given by

$$\mathcal{H} = 2\sqrt{6}J \Lambda_{A_1} - 4hM - 2J (\alpha_{A_1} \Lambda_{A_1} \rho_{A_1} + \alpha_E \Lambda_E \cdot \rho_E + \alpha_{T_2} \Lambda_{T_2} \cdot \rho_{T_2}) + (K_{A_1} \rho_{A_1}^2 + K_E \rho_E^2 + K_{T_2} \rho_{T_2}^2). \quad (3)$$

⁵ In general, the changes in bond length $\delta_{i,j}$ are not independent variables, but rather implicit functions of the positions of all the magnetic ions. However, since in this special four-sublattice case the lattice is subject to a uniform distortion (an affine transformation), the lengths of the six bonds making up the tetrahedron can be treated as independent quantities.

M is the average magnetization per site. The energy minima are found for $\rho_R = (\alpha_R J / K_R) \Lambda_R$, so the energy above becomes

$$\mathcal{H} = 2J \left(\sqrt{6} \Lambda_{A_1} - b_{A_1} \Lambda_{A_1}^2 - b_E \Lambda_E^2 - b_{T_2} \Lambda_{T_2}^2 \right) - 4hM \quad (4)$$

with $b_R = J\alpha_R^2 / (2K_R)$. Actually, for the simple model defined by equation (1), all the couplings turn out to be equal: $b_{A_1} = b_E = b_{T_2}$; and this is the case we have considered in [9]. This implied that only biquadratic terms of the form $(\mathbf{S}_i \cdot \mathbf{S}_j)^2$ were present in the Hamiltonian. Once we allow nonequal couplings, we get three- and four-site terms in the effective Hamiltonian of the form

$$\begin{aligned} \mathcal{H} = & 2J \sum_{i,j} \mathbf{S}_i \cdot \mathbf{S}_j - h \sum_i S_i^z - \frac{J}{3} (b_{A_1} + 2b_E + 3b_{T_2}) \sum_{i,j} (\mathbf{S}_i \cdot \mathbf{S}_j)^2 \\ & - \frac{2J}{3} (b_{A_1} - b_E) \sum_{i,j,k} (\mathbf{S}_i \cdot \mathbf{S}_j) (\mathbf{S}_j \cdot \mathbf{S}_k) \\ & - \frac{J}{3} (b_{A_1} + 2b_E - 3b_{T_2}) \sum_{i,j,k,l} (\mathbf{S}_i \cdot \mathbf{S}_j) (\mathbf{S}_k \cdot \mathbf{S}_l), \end{aligned} \quad (5)$$

where the summations are carried out such that every possible combination of spins in the tetrahedron appears exactly once; furthermore, $i \neq j \neq k \neq l$.

This result is of a very general nature: equation (4) is the most general Hamiltonian at fourth order in spin operators describing a four-sublattice long-range ordered state on the pyrochlore or fcc lattice. As such, it is independent of the actual origin of the coupling, which may equally be due to quantum and thermal fluctuations, or higher order exchange processes [10]. It could have been derived on purely phenomenological grounds, as the sum of the group invariants: $\Lambda_{A_1} = 8(M^2 - 1/4)/\sqrt{6}$ (and its powers) is itself invariant, while we can construct the quadratic forms $\Lambda_E^2 = \Lambda_{E,1}^2 + \Lambda_{E,2}^2$ and $\Lambda_{T_2}^2 = \Lambda_{T_2,1}^2 + \Lambda_{T_2,2}^2 + \Lambda_{T_2,3}^2$ from the E and T_2 irreps. There are six cubic invariants; three trivial ones $\Lambda_{A_1}^3$, $\Lambda_{A_1} \Lambda_E^2$, and $\Lambda_{A_1} \Lambda_{T_2}^2$, and three nontrivial ones $\Lambda_{E,1}^3 - 3\Lambda_{E,1} \Lambda_{E,2}^2$, $\Lambda_{T_2,1} \Lambda_{T_2,2} \Lambda_{T_2,3}$ and

$$\left(-\frac{1}{2} \Lambda_{E,1} - \frac{\sqrt{3}}{2} \Lambda_{E,2} \right) \Lambda_{T_2,1}^2 + \left(-\frac{1}{2} \Lambda_{E,1} + \frac{\sqrt{3}}{2} \Lambda_{E,2} \right) \Lambda_{T_2,2}^2 + \Lambda_{E,1} \Lambda_{T_2,3}^2.$$

These can also, in principle, be added to the Hamiltonian, but the resulting proliferation of parameters would make the problem intractable, and for that reason we neglect them here. All of the invariants considered above are constructed from two-spin dot products: at sixth order more complicated spin expressions may appear.

3. Stability analysis of the collinear states

Both the plateau and the fully polarized states are realized with collinear spin configurations, with spins pointing along the magnetic field. At certain critical values of magnetic field, these configurations cease to be favourable, and the spins cant to optimize their energy. This can be a continuous transition, when the magnetization smoothly changes from the fractional value, or a first order transition, in which case the magnetization jumps. Here we introduce a simple effective Hamiltonian to treat this effect, first for the fully polarized state, and then for the plateau.

3.1. Instability of the fully polarized state

Small fluctuations about the fully polarized state can be characterized by

$$\mathbf{S}_j = \left(\eta_j, \xi_j, \sqrt{1 - \eta_j^2 - \xi_j^2} \right), \quad (6)$$

where η_j and ξ_j are small. The η_j and ξ_j are site variables, which transform according to the A_1 and T_2 irreps⁶. Furthermore, since the model is isotropic, the magnetization always points along the magnetic field: $\sum_j \eta_j = \sum_j \xi_j = 0$. This means that the A_1 irrep is zero, and we need to worry about the T_2 irrep only. Apart from the space-group symmetry, the magnetic field reduces the $O(3)$ spin-symmetry to $U(1)$, the rotation of spins around the axis parallel to the magnetic field. Instead of the real η_j and ξ_j quantities it is useful to introduce the complex $\eta_j + i\xi_j$ quantity:

$$\begin{aligned} \eta_1 + i\xi_1 &= \mu_1 + \mu_2 + \mu_3, & \eta_3 + i\xi_3 &= -\mu_1 + \mu_2 - \mu_3, \\ \eta_2 + i\xi_2 &= \mu_1 - \mu_2 - \mu_3, & \eta_4 + i\xi_4 &= -\mu_1 - \mu_2 + \mu_3, \end{aligned} \quad (7)$$

where the complex $\boldsymbol{\mu} = (\mu_1, \mu_2, \mu_3)$ transforms according to the three-dimensional T_2 irrep.

Assuming a second order transition, the fully polarized state becomes unstable at a critical field of

$$h_F = 8J(1 - 2b_{A_1}). \quad (8)$$

Expanding to fourth order in $\boldsymbol{\mu}$ at this critical field, the energy per spin of the resulting canted state reads

$$\begin{aligned} E &= E_F + \frac{1}{2}(h - h_F)|\boldsymbol{\mu}|^2 + \frac{J}{3}(3 - 22b_{A_1} - 8b_E)|\boldsymbol{\mu}|^4 \\ &\quad + 8J(b_E - b_{T_2})(|\mu_1|^2|\mu_2|^2 + |\mu_1|^2|\mu_3|^2 + |\mu_2|^2|\mu_3|^2) \\ &\quad - 4Jb_{T_2}(\mu_1^2\bar{\mu}_2^2 + \bar{\mu}_1^2\mu_2^2 + \mu_1^2\bar{\mu}_3^2 + \bar{\mu}_1^2\mu_3^2 + \mu_2^2\bar{\mu}_3^2 + \bar{\mu}_2^2\mu_3^2), \end{aligned} \quad (9)$$

where $E_F = 3J(1 - b_{A_1}) - h$ is the energy of a spin aligned with the magnetic field. Minimizing this energy as a function of the coupling parameters we obtain the results shown in figure 2(a). In the clockwise direction, we observe four phases: (i) the coplanar 2:2 canted phase of E symmetry with $\boldsymbol{\mu} \propto (1, 0, 0)$ (and permutations) when $b_E > 0$ and $b_E > 2b_{T_2}$; (ii) the T_2 symmetric coplanar 3:1 canted state with $|\mu_1| = |\mu_2| = |\mu_3|$ and equal arguments modulo π for $b_{T_2} > 0$ and $b_E < 2b_{T_2}$; (iii) a T_2 symmetric umbrella-like configuration with $\boldsymbol{\mu} \propto (1, e^{\frac{2\pi i}{3}}, e^{-\frac{2\pi i}{3}})$ when $b_{T_2} < 0$ and $b_E < 2b_{T_2}$; (iv) an E symmetric 1:1:1:1 umbrella-like configuration with $\boldsymbol{\mu} \propto (1, \pm i, 0)$ when $b_E < 0$ and $b_E > 2b_{T_2}$.

The transition changes from a continuous into a first order one when the prefactor of the quartic term becomes negative. In the 2:2 phase, this happens for $8b_E > 3 - 22b_{A_1}$, while in the 3:1 state it happens for $16b_{T_2} > 3 - 22b_{A_1}$. Similarly, a first order transition takes place when $22b_{A_1} > 3 - 4b_{T_2}$ in case (iii) and $22b_{A_1} > 3 - 2b_E$ in case (iv).

3.2. Instability of the plateau

The analysis can be repeated for the stability of the plateau state: we assume that the spin at site 1 is down, $\mathbf{S}_1 = (\eta_1, \xi_1, -\sqrt{1 - \eta_1^2 - \xi_1^2})$, while the others (sites 2, 3 and 4) are up. Instabilities occur at

$$h_l = 4J(1 - 4b_{T_2}) \quad \text{and} \quad h_u = 4J(1 + 2b_{T_2}), \quad (10)$$

⁶ The bond variables, which are ‘squares’ of site variables, can transform as A_1 , E and T_2 (as the product $T_2 \otimes T_2 = A_1 \oplus E \oplus T_1 \oplus T_2$).

i.e. the plateau is stable for $h_1 < h < h_u$, assuming a continuous phase transition, and its width is $24b_{\tau_2}$. Clearly first order transitions, if they occur, will shrink the magnitude of the plateau. Let us consider what happens at the upper edge of the plateau. The selection of the position of the down-pointing spin breaks the symmetry in the μ vector, and in our case, the soft mode is the $\mu \propto (1, 1, 1)$ direction. It is convenient to introduce the new variables $\mu^\parallel = (\mu_1 + \mu_2 + \mu_3)/\sqrt{3}$, and the $\mu_1^\perp = (2\mu_1 - \mu_2 - \mu_3)/\sqrt{6}$ and $\mu_2^\perp = (\mu_2 - \mu_3)/\sqrt{2}$, where μ_1^\perp and μ_2^\perp are perpendicular to μ^\parallel . Keeping terms up to fourth order in μ (keeping the relevant quartic term only) reads

$$E = E_P - \frac{1}{4}(h - h_u)|\mu^\parallel|^2 + 12Jb_{\tau_2} (|\mu_1^\perp|^2 + |\mu_2^\perp|^2) + \frac{J}{12}(3 - 4b_{A_1} + 2b_{\tau_2})|\mu^\parallel|^4. \quad (11)$$

Here $E_P = -h/2 - 3Jb_{\tau_2}$ is the energy of the plateau. The instability is toward the 3:1 coplanar state, with the up spins having all equal canting angles. The continuous transition becomes first order once $3 - 4b_{A_1} + 2b_{\tau_2} < 0$. This is the same 3:1 canted coplanar state found as the instability of the fully polarized solution, and there is no reason to suppose that the two states are not connected with each other: in other words, there is no symmetry requirement for an additional phase transition when moving from the plateau to the fully polarized state⁷.

Next, let us consider what happens at the lower edge of the plateau: the energy is

$$E = E_P - \frac{1}{2}(h_1 - h) (|\mu_1^\perp|^2 + |\mu_2^\perp|^2) + 6b_{\tau_2}|\mu^\parallel|^2 + \frac{2J}{3} (4b_E + b_{\tau_2}) |\mu_1^\perp \bar{\mu}_2^\perp - \bar{\mu}_1^\perp \mu_2^\perp|^2 + \frac{J}{3}(3 - 4b_{A_1} - 8b_E - 24b_{\tau_2}) (|\mu_1^\perp|^2 + |\mu_2^\perp|^2)^2 \quad (12)$$

and, in contrast to what happened at the upper critical field h_u , the softening occurs in the two modes perpendicular to μ^\parallel . The $|\mu_1^\perp \bar{\mu}_2^\perp - \bar{\mu}_1^\perp \mu_2^\perp|^2$ term selects the relative phase of the μ_1^\perp and μ_2^\perp : $\mu_1^\perp = \pm i\mu_2^\perp$, and a T_2 symmetric umbrella-like canting is realized for $4b_E + b_{\tau_2} < 0$, while for $4b_E + b_{\tau_2} > 0$ the instability is against a degenerate coplanar canting (only the phase of the μ_1^\perp and μ_2^\perp is fixed; their relative amplitude μ_2^\perp/μ_1^\perp is not). In fact we need to go to sixth order to select the 2:1:1 state of mixed E and T_2 symmetry previously found numerically [9]. This has three solutions: $(\mu_1, \mu_2) \propto (1, 0)$, or $(-1/2, \pm\sqrt{3}/2)$. These transitions become first order when $22b_{\tau_2} > 3 - 4b_{A_1}$ for the umbrella state, and when $8b_E + 24b_{\tau_2} > 3 - 4b_{A_1}$ for the 2:1:1 state (see figure 2(c)).

4. Extrema of the invariants and magnetization curves

Any given magnetization can be realized by a large number of (continuously degenerate) spin configurations. Within our model, the energy of these states is uniquely determined by the second order invariants Λ_R^2 . Therefore, by mapping out the extrema of these invariants, we exhaust all possible ground states selected by four spin interactions b_R . Doing so enables us not only to confirm the results of the stability analysis above, but to make some further observations about the magnetization process $M(h)$ and possible first order transitions.

Let us first consider the limiting case $\Lambda_{T_2}^2 = 0$. Then, from equation (2), the exchange energy on the opposing bonds of the tetrahedron is equal. This condition is satisfied by spins with equal S^z components, and the $(S^x, S^y) = (\pm 1, 0)$ and $(\pm \cos \phi, \pm \sin \phi)$. The maximum value of Λ_E^2 is obtained for a 2:2 canted state with $\phi = 0$, while the minimum is obtained for a fully symmetric 1:1:1:1 canting with $\phi = \pi/2$ (see figure 3), such that

$$\frac{4}{3}(1 - M^2)^2 \leq \Lambda_E^2 \leq \frac{16}{3}(1 - M^2)^2. \quad (13)$$

⁷ This need not be the case if we consider ordered states with more than four spins in the unit cell.

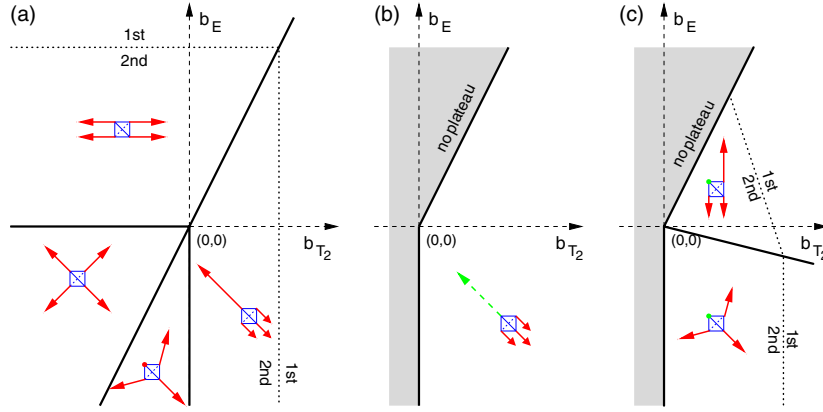


Figure 2. Instability of the (a) fully polarized state, and of the plateau at the (b) upper critical field h_u and (c) lower critical field h_l . The magnetic field is perpendicular to the plane, and the (red) arrows shows the spin canting (η_j, ξ_j) of the j th spin. Dots (green) and dashed arrows represent the down-pointing spin in (b) and (c), while the shaded grey region shows where the plateau is not present.

Next, let us consider the case of $\Lambda_E = 0$. The maximum value for $\Lambda_{T_2}^2 = 6$ is realized when all the $\Lambda_{T_2,i}$ take their maximal value $\Lambda_{T_2,i} = \sqrt{2}$ in the collinear uuud (three up-spins, one down-spin) configuration with $M = 1/2$. For $M > 1/2$, $\Lambda_{T_2}^2$ is maximal for the coplanar 3:1 canted state. For $M < 1/2$ the maximal state is a three-dimensional inverted umbrella-type configuration ($\mathbf{S}_j = (\sin \vartheta \cos[j2\pi/3], \sin \vartheta \sin[j2\pi/3], \cos \vartheta)$ for $j = 1, 2, 3$ and $\mathbf{S}_4 = (0, 0, -1)$), while the minimal state is obtained by inverting \mathbf{S}_4 to obtain a folded umbrella configuration, and

$$\frac{32}{3}M^2(1 - M)^2 \leq \Lambda_{T_2}^2 \leq \begin{cases} \frac{32}{3}(1 - M^2)^2, & \text{if } 1/2 \leq M \leq 1; \\ \frac{32}{3}M^2(1 + M)^2, & \text{if } 0 \leq M \leq 1/2. \end{cases} \quad (14)$$

However, a slightly better energy can be obtained by allowing finite values for Λ_E^2 , in which case the extremal point corresponds to coplanar 2:1:1 canted state with a relatively complex analytic form.

The existence and stability of the plateau is related to the cusp of $\Lambda_{T_2}^2$ at $M = 1/2$. As a singular point, it will minimize the energy for a finite window of the magnetic field when $2b_{T_2} > \max(b_E, 0)$, also allowing for negative values of b_E . This is in agreement with the results of the stability analysis presented above. The extrema in the $(\Lambda_E^2, \Lambda_{T_2}^2)$ plane can clearly be related to the nature of instability of the plateau and the fully polarized state.

However, we can also see that for $b_E > \max(2b_{T_2}, 0)$ the T_2 order is not realized at all (here we allow for negative values of b_{T_2}). The system remains in the coplanar 2:2 phase for all values of applied field up to saturation. The half-magnetization plateau is also absent when both b_E and b_{T_2} are negative: the ground state in this case is a noncoplanar spin configuration. It is also possible to achieve a T_2 -type solution for small field, and an E-type configuration for high field, with a first order transition between them.

In figure 1(b) we show the magnetization curve for a physically relevant set of parameters. To facilitate comparison with the experimentally measured curves, it is useful to extract the characteristic features of the magnetization curve. The energy per site of the 2:2 canted E

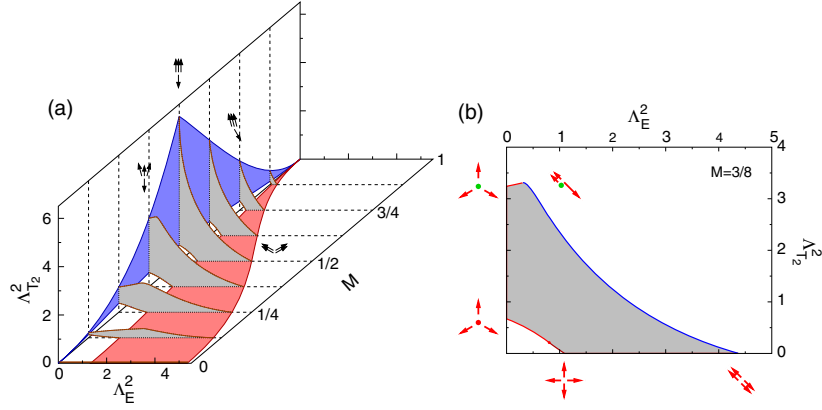


Figure 3. (a) The extremal values of Λ_E^2 and $\Lambda_{T_2}^2$ as a function of the magnetization M . (b) The cut at $M = 3/8$. The degenerate manifold maps into the shaded region, and the border is outlined in blue for coplanar and red for non-coplanar states. The spin configurations are shown from the direction of the magnetic field, with red arrows canted in the direction of the field, and the green dots represent spins pointing opposite to the field.

symmetry state is

$$E_{2:2} = -hM - J(1 - 4M^2) - \frac{J}{3}(1 - 4M^2)^2 b_{A_1} - \frac{8J}{3}(1 - M^2)^2 b_E \quad (15)$$

with zero field susceptibility

$$\left. \frac{\delta M}{\delta h} \right|_{h=0} = \frac{3}{8J} \frac{1}{3 + 2b_{A_1} + 4b_E}. \quad (16)$$

Similarly, the energy of the 3:1 canted state for $M \geq 1/2$ is

$$E_{3:1} = -hM - J(1 - 4M^2) - \frac{J}{3}(1 - 4M^2)^2 b_{A_1} - \frac{16J}{3}(1 - M^2)^2 b_{T_2}, \quad (17)$$

with differential susceptibility at the upper critical field

$$\left. \frac{\delta M}{\delta h} \right|_{h=4J+8b_{T_2}} = \frac{3}{8J} \frac{1}{3 - 4b_{A_1} + 2b_{T_2}}. \quad (18)$$

If we continue the tangent of the magnetization curve at the upper critical field h_u of the plateau, it will cut the $M = 0$ axis at $h = 16J(b_{A_1} + b_{T_2})/3$ (Δh_1 in figure 1(b)). Similarly, if we continue the linear magnetization at low field, it will intersect the plateau at a distance $\Delta h_2 = 8J(3b_{T_2} - b_{A_1} - 2b_E)/3$ from h_u . These values are easily extracted from the experimentally measured magnetization curves, and together with the upper critical field for the plateau, (10), allow us to make a rough estimate of the strength of these parameters. Clearly, the cubic and higher order invariants will influence these results, and could also be used to fine tune the magnetization curve. Furthermore, experimental evidence points towards a more complicated, 8- [11] or 16-sublattice [12] ordered state, which is not described by this study. However, our preliminary results on the 16-sublattice state seem to indicate that the shape of the magnetization curve may remain the same even in the case of 8- and 16-sublattice ordering in certain (possibly relevant) cases, where the b_R parameters of the invariants of the T_d group are replaced by the appropriate coupling constant of the invariants of the larger point group.

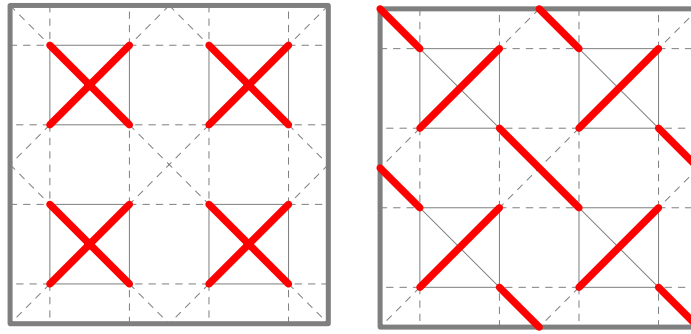


Figure 4. Possible valence bond configurations which do not break translational symmetry.

5. Extreme quantum case

In this paper we have concentrated on classical spins. What changes when we take into account the quantum nature of the spins? When the spins are ordered, we expect some corrections to the theory coming from quantum fluctuations (which are in fact effectively taken into account by the b_R terms [10]). However, in the spin-1/2 quantum limit, it may happen that spins choose to form singlets, rather than ordering magnetically (similar physics for spin-1 has been studied in [4]). Even though the unit cell of the ordered state remains the four-site unit cell, we need to extend our theory to take into account the inversion symmetry I broken by singlet bonds. We therefore need to classify the bond parameters according to the irreps \mathbb{R}' of the cubic group $\mathcal{O}_h = \{1, I\} \otimes \mathcal{T}_d$. Having done so, we can write an effective energy in terms of the $\Lambda_{\mathbb{R}'}^2$. For zero magnetization, the possible valence bond patterns are shown in figure 4: when $b_{A_{2u}} + 2b_{E_u} > 3b_{T_{1u}}$,⁸ the valence bonds occupy alternate tetrahedra, otherwise they form a single valence bond in tetrahedron, with exchange energy distributed evenly among the tetrahedra.

6. Conclusions

In this paper, we have presented a complete symmetry analysis of all possible four-sublattice phases of a classical pyrochlore antiferromagnet in applied magnetic field, and determined its magnetic phase diagram for the most general four-spin interactions. This theory captures the essential physics of spin–lattice coupling in spinel and pyrochlore materials, and provides considerable insight into the magnetization plateaus observed in Cr spinels. In a separate publication, we will consider the new complexities which arise when this symmetry analysis is generalized to the full 16-site *cubic* unit cell of the pyrochlore lattice [13].

Acknowledgments

We are pleased to acknowledge helpful discussions with M Hagiwara, H A Katori, H Takagi and H Ueda. This work was supported by the Hungarian OTKA Grants Nos. T049607 and K62280, and EPSRC grant EP/C539974/1 and Grant No. 16GS0219 from the Ministry of Education, Japan, as well as the HAS-JSPS bilateral project. KP and NS are also grateful for the hospitality of MPI–PKS Dresden, where a large part of this work was completed.

⁸ Using the standard notation for the irreps of the \mathcal{O}_h . The irreps \mathbb{R} of the \mathcal{T}_d become $\mathbb{R}' = \text{Rg}$ of the \mathcal{O}_h .

References

- [1] Moessner R and Chalker J T 1998 *Phys. Rev. B* **58** 12049
Moessner R and Chalker J T 1998 *Phys. Rev. Lett.* **80** 2929
- [2] Canals B and Lacroix C 2000 *Phys. Rev. B* **61** 1149
Canals B and Lacroix C 1998 *Phys. Rev. Lett.* **80** 2933
- [3] Tchernyshyov O, Moessner R and Sondhi S L 2002 *Phys. Rev. Lett.* **88** 067203
Tchernyshyov O, Moessner R and Sondhi S L 2002 *Phys. Rev. B* **66** 064403
- [4] Yamashita Y and Ueda K 2000 *Phys. Rev. Lett.* **85** 4960
- [5] Terao J 1996 *J. Phys. Soc. Japan* **65** 1413
- [6] Keren A and Gardner J S 2001 *Phys. Rev. Lett.* **87** 177201
- [7] Ueda H, Katori H A, Mitamura H, Goto T and Takagi H 2005 *Phys. Rev. Lett.* **94** 047202
- [8] Ueda H, Mitamura H, Goto T and Ueda Y 2006 *Phys. Rev. B* **73** 094415
- [9] Penc K, Shannon N and Shiba H 2004 *Phys. Rev. Lett.* **93** 197203
- [10] Nikuni T and Shiba H 1993 *J. Phys. Soc. Japan* **62** 3268
Shiba H, Nikuni T and Jacobs A E 2000 *J. Phys. Soc. Japan* **69** 1484
- [11] Chung J H, Matsuda M, Lee S H, Kakurai K, Ueda H, Sato T J, Takagi H, Hong K P and Park S 2005 *Phys. Rev. Lett.* **95** 247204
- [12] Ueda H, private communication
- [13] Penc K *et al* 2006 in preparation